

High-top clouds play an efficient part in moisture transport to the Antarctic

Kazue Suzuki¹, Terumasa Tokunaga², Takashi Yamanouchi³, and Hideaki Motoyama³

¹Hosei University

²Kyushu Institute of Technology

³National Institute of Polar Research

November 21, 2022

Abstract

We verified high-top clouds from satellite imaging that contributed to snow accumulation at Syowa Station, Antarctica, during a blizzard event in 2009. Snow stake data shows that the accumulation recorded in 2009 and 2011 increased during 1993–2012 through the traverse route in East Antarctica. Focusing on 2009 events, the high-top cloud structure in the stitched satellite image was often linked to the atmospheric river (AR) and the values for the high-top cloud area. We found seven new AR events for 2009 with high accumulations and high-top cloud (HTC) areas. After comparing the HTC area to precipitable water and integrated water vapor transport, we determined that the selected cloud images can be used as a parameter for snowfall. This paper introduces a new fusion method for identifying AR using image analysis and in-situ glacial and meteorological data. These HTC clouds are beneficial for predicting the accumulation in the future.

1 **High-top clouds play an efficient part in moisture transport to the Antarctic**

2

3 **Kazue Suzuki¹, Terumasa Tokunaga², Takashi Yamanouchi³, and Hideaki Motoyama³**

4 ¹Hosei University

5 ²Kyushu Institute of Technology

6 ³National Institute of Polar Research

7 Corresponding author: Kazue Suzuki (kazue.suzuki.88@hosei.ac.jp)

8 **Key Points:**

9 High-top clouds from satellite imaging analysis contributed to the accumulation of snow at Syowa
10 Station, Antarctica in a blizzard in 2009.

11 Seven new atmospheric river events were found in 2009 with high accumulations and high-top
12 cloud areas, three events detected by previously.

13 Compared with precipitable water and integrated water vapor transport, the cloud detected can be a
14 parameter for predicting an accumulation.

15 **Abstract**

16 We verified high-top clouds from satellite imaging that contributed to snow accumulation at
17 Syowa Station, Antarctica, during a blizzard event in 2009. Snow stake data shows that the
18 accumulation recorded in 2009 and 2011 increased during 1993–2012 through the traverse route in
19 East Antarctica. Focusing on 2009 events, the high-top cloud structure in the stitched satellite
20 image was often linked to the atmospheric river (AR) and the values for the high-top cloud area.
21 We found seven new AR events for 2009 with high accumulations and high-top cloud (HTC)
22 areas. After comparing the HTC area to precipitable water and integrated water vapor transport,
23 we determined that the selected cloud images can be used as a parameter for snowfall. This paper
24 introduces a new fusion method for identifying AR using image analysis and in-situ glacial and
25 meteorological data. These HTC clouds are beneficial for predicting the accumulation in the
26 future.

27 Keywords: surface mass balance, satellite image, image analysis, atmospheric river

28

29 **Plain Language Summary**

30 We verified that the high-top cloud from satellite imaging contributed to snow accumulation at
31 Syowa Station, Antarctica, in the blizzard of 2009. From the snow stakes data, the accumulation in
32 2009 and 2011 increased during 1993–2012 through the traverse route in East Antarctica.
33 Focusing on the events in 2009, the high-top cloud structure in the stitched satellite image often
34 linked the atmospheric river and the values of the high-top cloud area; the heavy snow conditions
35 differed from the light snow conditions. Finally, we found the seven atmospheric river events in
36 2009 with high accumulations and high-top cloud areas. Precipitable water calculated by radio
37 sonde data indicated the AR clouds had a higher HTC area than non-AR. This result was reflected

38 that the AR is a narrower long moisture band, and the cloud area should expand. We found that the
39 IVT of our AR events exceeded three times of standard deviation of a monthly threshold. The
40 above results indicated that the cloud detected can be a parameter for predicting an accumulation.
41 This method is new for finding moisture transport to the Antarctic.

42

43 **1 Introduction**

44 Recently, variation in the surface mass balance (SMB) has attracted substantial interest
45 because it strongly influences the sea level rise. Based on satellite observations, the loss of SMB
46 around the West Antarctic ice sheet with increasing temperature has been reported for decades
47 (Bromwich et al. 2013; Fernando et al. 2015; Zwally et al., 2015). To capture the correct SMB
48 variation, the processes of accumulation by precipitation, and consumption by runoff,
49 sublimation/evaporation, erosion need to be understood, with further observations being required.
50 The precipitation has an important role on the accumulation because the only phenomena to
51 recharge the icesheet. However, severe environments and snowdrifts make in-situ observation of
52 snowfall events challenging. Given that the snowfall amount provided by several reanalysis
53 datasets and regional climate models show are inconsistent with the observed snowfall event
54 around the Syowa Station (Agosta et al. 2019), it is important to verify that the elements from the
55 reanalysis data are sufficient for interpreting snowfall events. The Japanese Antarctic Research
56 Expedition (JARE) has observed the snow stake data along the traverse route from the Syowa to
57 the Dome Fuji stations from 1992 to the present (Figure 1, data from Motoyama et al., 2008;
58 Motoyama et al., 2015). These data have captured the net interannual accumulation from the
59 coastal to the interior regions around East Antarctica (Figure 1b). Interannual accumulation
60 increased during the late 2000s, especially in the coastal region. The variation of katabatic area

61 accumulation and adding up snow depth at Syowa Station increased around 2009, however, the
62 coastal area accumulation decreased conversely. In 2009, a substantial amount of snowfall was
63 observed in East Antarctica, including at the Princess Elisabeth Station and Syowa Station, and the
64 moisture transport was analyzed (Gorodetskaya et al., 2014). The atmospheric river (AR) in front
65 of a cyclonic disturbance enhanced the poleward moisture flux outside Antarctica and carried
66 substantial snowfall into the region. The blizzard events that occur at the Syowa Station often
67 exhibit similar atmospheric circulation conditions (Sato & Hirasawa, 2007). The interannual
68 variation of SMB focusing on the coastal area shows that the increasing trend of SMB in the late
69 2000s peaked in 2011 and turned to decrease. Here, we target the events in 2009, the same as in
70 Gorodetsukaya et al. (2014), to verify the water vapor transport by AR at Syowa Station.

71

72 (a) The map of East Antarctica and the Japanese Antarctic Research Expedition's traverse.

73

74

75

76

77

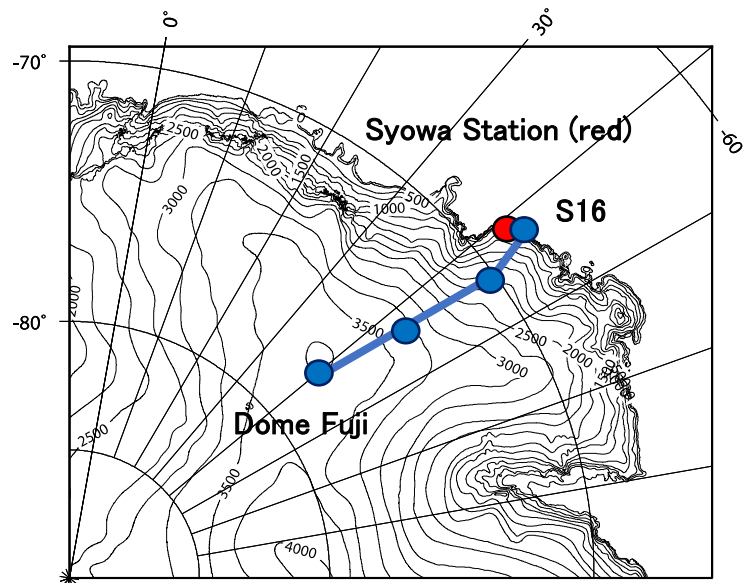
78

79

80

81

82 (b)



96 snowfall amount in the coastal region, we cannot exclude the effects of wind-driven snow erosion
97 and deposition.

98 Here, we investigate the relationship between the observed atmospheric elements and
99 cloud patterns from satellite data such as AR to clarify the explanatory variables in estimating the
100 snowfall amount. We have constructed a new convolutional neural network (CNN) architecture to
101 automatically identify the high-height clouds associated with the AR (Suzuki et al., 2021). If the
102 snowfall amount or snow accumulation can be estimated based on the in-situ and satellite observed
103 and reanalysis data, we can estimate the SMB for the entire Antarctic ice sheet under the present
104 climate. This method can play a key role in the adaptation of other meteorological and ice sheet
105 fluid modeling for application in the context of past and future climates.

106

107 **2 Detection of the high height cloud area**

108 In this study, we used NOAA/AVHRR images (for the infrared band, channel 4) that had
109 been received at Syowa Station. Due to polar orbit satellite observations, the field of vision in the
110 images changed several times each day. Contamination often occurs during blizzard events with
111 heavy storms because their strong winds and snowfall cause electromagnetic interferences from
112 receiving data from the satellites. We stitched several images to analyze the wider cloud structure.
113 The stitching condition is the duration before or after six hours from the observation and using an
114 averaged pixel brightness for overlap area. After the images had been stitched, the HTC area was
115 detected. We made a mask of the land area in the image by using only the over sea or the sea ice
116 area. We then applied image binarization using local thresholding with a pixel brightness of 100
117 and image erosion three times. After this, we estimated the contour of the HTC using the Chan–
118 Vese segmentation algorithm (Chan & Vese, 1999). In Figure 2, we show an example of the

119 stitched image (upper) and estimated area as HTC, and the red-line enclosure is the HTC area in
120 the image (lower). Gorodetskaya et al. (2014) highlighted that there were deep troughs following
121 cyclonic disturbance and direct moisture transport with polar ward flux were enhanced for the ice
122 sheet (they called them ARs). The area detected in Figure 2 is likely to be in the same condition as
123 AR. The definition of HTC including the top level of storm convection should be over 500 hPa and
124 could potentially reach 300 hPa by chance.

125

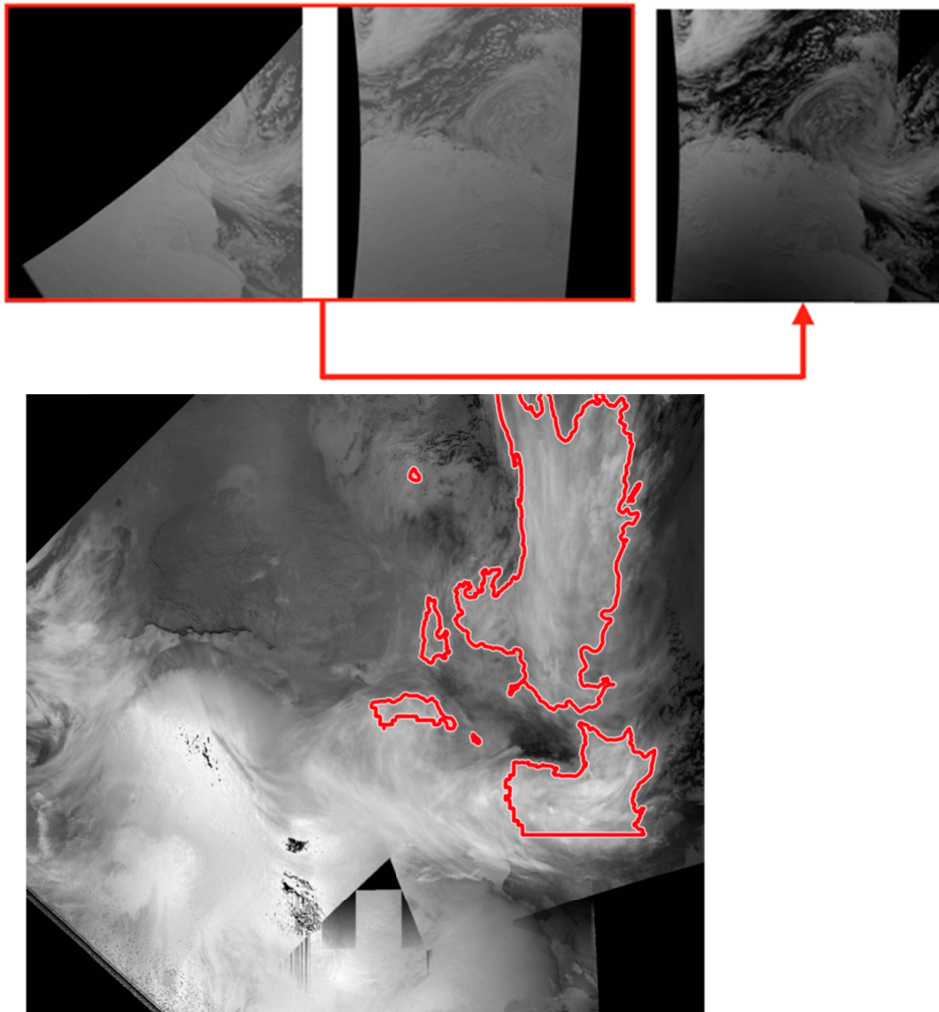
126

20090228.1315.n18.hrpt.ch1 20090228.0953.n18.hrpt.ch1

127

128

129



130

131 **Figure 2.** (Upper) The merging process for the satellite images from two pieces. (Lower) Sample
132 merged image and the area surrounded by red lines have high brightness temperatures that we have
133 called HTC.

134

135 **3 Analysis of Blizzard Events**

136 JARE has operated in-situ meteorological observations over a long time. The surface
137 observations include pressure, temperature, wind speed, wind direction, weather conditions, and
138 the amount of cloud at Syowa Station from February 1957 to the present. Blizzards often occur
139 with severe snowstorms, with approximately 25.1 blizzard events at Syowa per year on average
140 (Sato & Hirasawa, 2007). The in-situ weather conditions were observed as snowfall in all blizzard
141 events for 2009. In this paper, these blizzard events were designated as snowfall events because the
142 blizzard is connected with the heavy storms such as the AR analyzed by Gorodetskaya et al.
143 (2014). We have only focused on the events in 2009 because the accumulation increasing as shown
144 in Figure 1b and the number of blizzards were 28 and more than average, that mean we have large
145 sample size. The criteria have three blizzard grades. Here, we have disregarded the differences
146 between the blizzard grades. However, A-grade blizzards with wind speed over 15 m/s and
147 visibility under 100 m can be treated as severe snowstorms. The structure and the number of
148 clouds with snowfall were analyzed. We compared the heavy snow clouds with light snow clouds
149 based on the snow depth data from Syowa Station. The snow depth was observed using an
150 electronic snow gage and the data were sent by radio. During the blizzard event, the heavy storm
151 made the winds considerably stronger. There was often a lack of snow depth data, especially under
152 storm conditions because of there being weak reception at the station. The one of most simple
153 method to supplement the lack of snow depth data is to employ a time-series analysis. We

154 employed Kalman filtering, is a filtering method based on Bayesian inference using Gaussian
155 probabilities, to predict a time variation of snowfall amount. After filling the gaps in the dataset
156 with predicted values, we compared the pixels within the HTC area for different snow depth
157 conditions.

158 Figure 3 shows the HTC area maps for the different snow depth conditions. On the left is
159 the merged image with the maximum snow depth of 23 cm shown as a heavy snowfall event. The
160 HTC area is counted using the pixels. The area with heavy snowfall is 395 154 pixels, and the
161 trained HTC brought rich moisture from the mid-latitude in front of the cyclonic disturbance. The
162 position of the disturbance is quite important, with the synoptic atmospheric circulation pattern
163 having a characteristic pattern in the snowfall at Syowa Station. The main disturbances are west of
164 the station, and moisture transport is enhanced toward the ice sheet. The same situation was
165 identified by Sato and Hirasawa (2007) and Suzuki et al. (2008). However, under light snow
166 conditions, the cloud and disturbance patterns are similar to those of the snowfall. The pixels of the
167 HTC were 85 410, and smaller than those to the left of Figure 3. Using reanalysis meteorological
168 data and analyzing these situations, we were unable to make the characteristic patterns of the
169 elements clear. This method can effectively classify the amount of snowfall and accumulation,
170 which suggests that HTC such as AR substantially influences moisture transport to the Antarctic
171 and snowfall accumulation on the ice sheet.

172

173

174

175

176

177

178

179

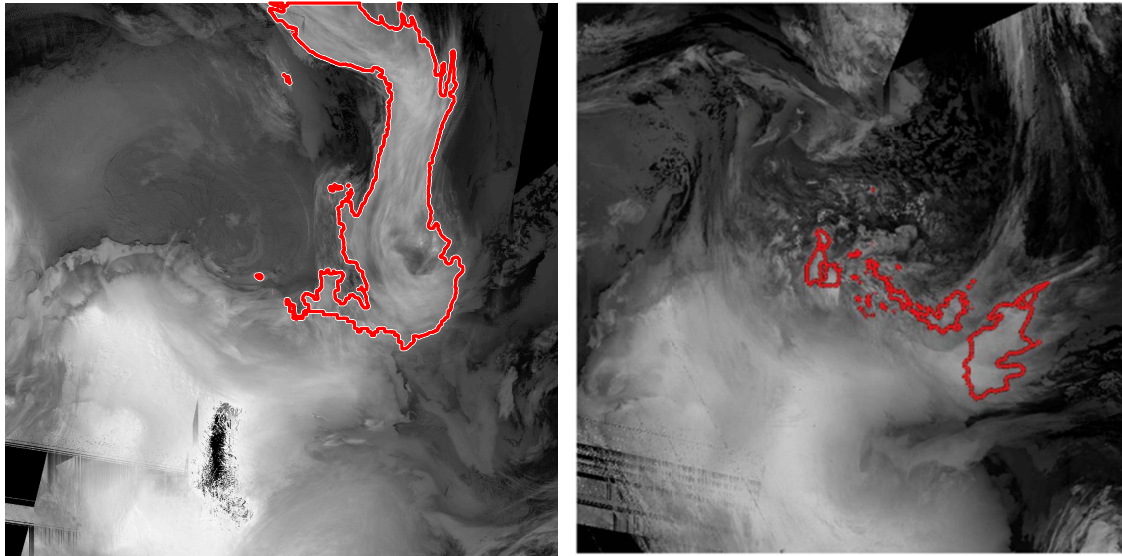
180

181

182

183

184



185 **Figure 3.** The merged satellite images under heavy (left) and light (right) snow conditions.

186

187 **4 Results and Discussion**

188 Figure 4 shows the time series of the snow depth and the duration of the blizzards, with the

189 red duration being for an A-grade blizzard. The duration is irrelevant to the variation in the snow

190 depth. Under blizzard conditions, in some cases, the snow depth has increased or decreased with

191 no change in the quantities. Given that our final goal is to estimate the surface mass balance of

192 Antarctica, we chose an event with increasing snow depth. The snowfall was confirmed by

193 observation and the snow depth increased. The event was detected as AR based on the conditions

194 with the clouds being over Syowa Station and that the clouds were persistent over a long distance.

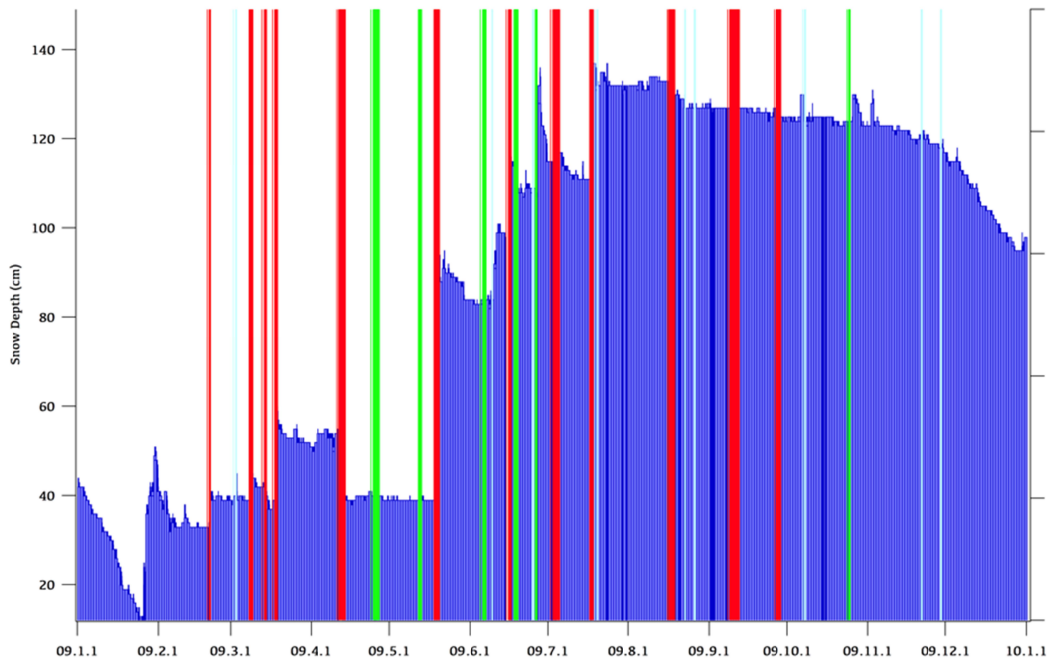
195 It is important to validate the events that were detected using HTC and the snow depth in

196 the context of moisture transport to the Antarctic. The difference between events was initially

197 investigated by calculating the amount of precipitable water from radiosonde data at the time of the

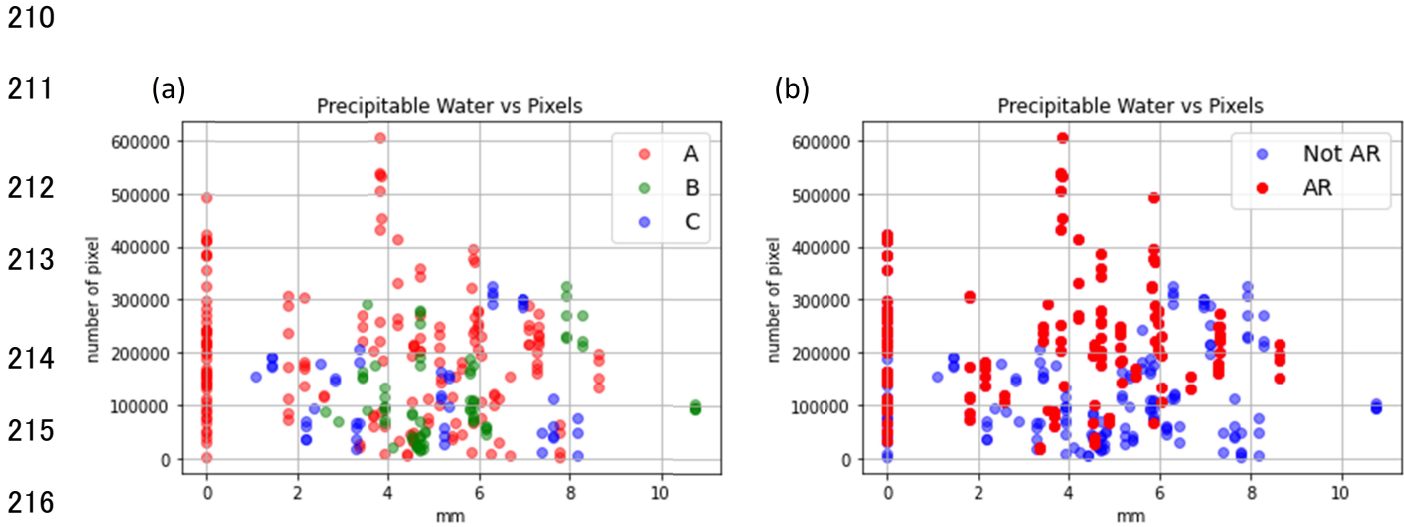
198 observation. In this case, the precipitable precipitation is the integrated value up to the altitude
 199 where the temperature does not fall below $-40\text{ }^{\circ}\text{C}$. Figure 5(a) shows a plot of cloud area versus the
 200 precipitable water for each blizzard class. The precipitable precipitation is zero because it cannot
 201 be calculated due to the missing measurements. The red, green, and blue areas indicate the cloud
 202 area for the Grade A, B, and C blizzards, respectively, and all the missing measurements were
 203 taken during the Grade A blizzard. Figure 5(b) shows the number of cloud areas for ARs (red) and
 204 others (blue), regardless of the grade. The number of cloud areas as a snapshot could potentially be
 205 significant.

206



207

208 **Figure 4.** The snow depth at Syowa Station in 2009 (blue) and the strength of the blizzard (Grade
 209 A is red, Grade B is green, and pale blue is for Grade C).



217 **Figure 5.** (a) Distribution of precipitable water at Syowa Station and the number of HTC pixels.
 218 Color differs from the blizzard grades. When observation data is lacking, the precipitable water
 219 equals zero. (b) The precipitable water at Syowa Station and the number of HTC pixels have the
 220 same distribution but the colors show whether an AR event has occurred.

221

222 Based on the definition of HTC, we identified seven AR events with high accumulations and
 223 the HTC area from all the blizzards in 2009 at Syowa Station (Table 1, 10 events). The specific AR
 224 events indicated by Gorodetskaya et al. (2014) were also confirmed at Syowa Station (right
 225 column of Table 1, three of ten events). The stations are near each other in the Droning Maud Land
 226 and the synoptic-scale disturbances often have the same effect on the SMB. In the highest
 227 accumulation event, the snowstorm resulted in an accumulation of 43 cm from 18 May to 20 May,
 228 and the maximum snow depth in 2009 was 135 cm. During that event, over 30% of the amplitude

229 for the year had accumulated. The mean HTC area for the blizzard was 191 484 pixels and the
230 maxima was 323 297 pixels. Approximately 5 cm of snow depth can be brought by clouds without
231 many HTCs. The correlation is 0.3 between the snow depth and pixels but the possibility of high
232 accumulation can be interpreted.

233 The next step was calculating the IVT (Mundhenk et al., 2016) using objective
234 meteorological data (ERA5 hourly data on pressure levels from 1959 to present, Hersbach, H. et
235 al., 2018) to detect cloud features as ARs. It is difficult to calculate the specific humidity up to 300
236 hPa using radiosonde data due to the temperature problem. Therefore, it is necessary to use
237 objective analysis data and to compare the results with those obtained using radiosonde
238 observations. ERA5 is the best reanalysis meteorological data at temperature and accumulation in
239 the Antarctic (Gossart et al. 2019). Here, we used Integrated Water Vapor Transport (IVT,
240 Mundhenk et al. 2016) as the AR threshold. Using ERA5, we obtained the time-series of IVT for
241 each month for Syowa Station in 2009. With a threshold (three times of monthly standard
242 deviation; 3σ as 0.99%) confidential, we could recognize the detected AR events as rare events to
243 find the atmospheric river and the large amount of snowfall. We examined all of AR events shown
244 in Table 1 using IVT. Finally, eight of the 10 events exceeding the monthly threshold (3σ) were
245 found and at least two events were exceeding the monthly threshold (2σ). However, the maximum
246 for IVT at Syowa Station in 2009 was $140.33 \text{ kg m}^{-1}\text{s}^{-1}$ and did not exceed the anomalous AR
247 threshold ($250 \text{ kg m}^{-1}\text{s}^{-1}$). Because the moisture in the polar region is relatively lower than that in
248 the low and mid latitudes, it is likely that AR does not require a rich water vapor to occur and
249 maintain its structure around the Antarctic. Gorodetsukaya et al. (2014) introduced a new equation
250 for IVT adapted to the polar region, however, we have confidence that HTC with satellite image
251 can take a role to detect the AR and anomalous accumulation event.

252

253 **Table 1.** The AR events were detected using the proposed method from the blizzard at
254 Syowa Station in 2009. “N” means the serial number for the blizzard events.

255

AR event identified by our methodology			AR event identified by our methodology as same as analyzed by Gorodetsukaya et al. (2014)		
n	start time	end time	n	start time	end time
4	2009/3/13 21:50	2009/3/14 18:15	9	2009/5/18 3:50	2009/5/20 3:05
16	2009/7/2 21:50	2009/7/5 12:20	12	2009/6/15 19:30	2009/6/16 21:50
18	2009/7/17 3:10	2009/7/18 10:10	17	2009/7/5 13:20	2009/7/7 17:40
20	2009/8/16 12:50	2009/8/18 21:28			
23	2009/9/8 19:00	2009/9/12 12:50			
24	2009/9/26 17:10	2009/9/28 14:55			
26	2009/10/24 15:40	2009/10/25 5:50			

256

257

258

259

260

261

262

263

264

265

266

267

For undertaking research on past climates, many ice cores obtained from Antarctica were analyzed and they predicted the past atmospheric circulation and moisture transport to the ice sheet (Buizert et al., 2018). Determining the origin of the moisture transport is critical to understand the variation in deuterium-excess records as the surface temperature. The distribution of the modeled moisture sources for the Dome Fuji ice core is similar to the AR in this study around Syowa Station and the ocean area close to Syowa. This AR condition can also bring moisture to the interior region which can accumulate. In the backward trajectory analysis using reanalysis meteorological data, we found many tracks such as AR that directly impacted the station. This means that moisture transport from the mid-latitude is enhanced and moves poleward as the AR occurs during the development of cyclonic disturbances, and the snowfall accumulated directly on the ice sheet. The amount of snowfall cannot currently be simulated. We have confirmed that HTC contributes to the

268 accumulation or decrease of snow on the ice sheet. In the further work, the SMB can be solved as
269 stochastic model with HTC and snow depth, and some meteorological parameters. Our final goal
270 is a coupling between CNN to find AR and stochastic model to predict accumulation for whole
271 Antarctica.

272 **5 Conclusion**

273 Using satellite images, we verified that AR events associated the HTC contributed to the
274 accumulation at Syowa Station, Antarctica in the blizzards for 2009. The detected HTC structure
275 in the stitched satellite image with imaging analysis method often linked the AR and the values of
276 the HTC area, and in the heavy snow conditions, they were different from the light snow
277 conditions. We found the new seven AR events in 2009 with high accumulations and the HTC area
278 at Syowa Station as well as three same events of Gorodetsukaya et al. (2014) with IVT method. As
279 in other stations in the Droning Maud Land, high accumulate events were confirmed in May at
280 Syowa Station. The snowstorm with the HTC area can affect the high accumulation of more than
281 10 cm of snow depth. Precipitable water calculated by radio sonde data indicated the AR clouds
282 had a higher HTC area than non-AR. This result was reflected that the AR is a narrower long
283 moisture band, and the cloud area should expand. We found that the IVT of our AR events
284 exceeded three times of standard deviation of a monthly threshold. Detected ARs with high HTC
285 area were satisfied as anomalous accumulation events. However, in the polar region, the IVT for
286 AR should be treated as the different measure from low - mid latitudes. This is a new fusion
287 method for finding moisture transport to the Antarctic using image analyzing method and in-situ
288 glacial and meteorological data and can be a prototype for adapting machine leaning and stochastic
289 method.

290

291 **Acknowledgements**

292 This work was supported by ROIS-DS-JOINT (009RP2019, 035RP2022) and JSPS
293 KAKENHI Grant Number 16K21585, 20K11718. Naohiko Hirasawa from National Institute of
294 Polar Research was very helpful for using NOAA/AVHRR data and commented on the treatment
295 for snow depth and radio sonde data. All of meteorological observation data were offered by Japan
296 Meteorological Agency. The results contain modified Copernicus Climate Change Service
297 information 2020. Neither the European Commission nor ECMWF is responsible for any use that
298 may be made of the Copernicus information or data it contains.

299

300 **Open Research**

301 The NOAA/AVHRR infrared channel brightness temperature data are available,
302 https://www.avl.class.noaa.gov/saa/products/search?datatype_family=AVHRR. The provided
303 data are HRPT type, so we introduce a site where you can see quick-look images. The National
304 Polar Research Institute archives the converted images in this repository,
305 https://scidbase.nipr.ac.jp/modules/metadata/index.php?content_id=121; doi acquisition is in
306 progress. Snow depth data along the JARE traverse route are shown in Motoyama et al. (2015),
307 <https://doi.org/10.15094/00010905>. Hourly snow depth data at Syowa Station are available from
308 the Japan Meteorological Agency, <https://www.data.jma.go.jp/gmd/risk/obsdl/index.php> (only
309 Japanese). Three-hourly present weather and three-hourly cloud amount at Syowa Station are
310 available from the Japan Meteorological Agency,
311 <https://www.data.jma.go.jp/antarctic/datareport/index-e.html>. ERA5 hourly data on pressure
312 levels from 1959 to present (Hersbach, H. et al. 2018) was downloaded from the Copernicus
313 Climate Change Service (C3S) Climate Data Store, <https://doi.org/10.24381/cds.bd0915c6>.

314

315 **References**

- 316 Agosta, C., Amory, C., Kittel, C., Orsi, A., Favier, V., Gallée, H., van den Broeke, M. R., Lenaerts,
317 J. T. M., van Wessem, J. M., van de Berg, W. J., & Fettweis, X. (2019), Estimation of the Antarctic
318 surface mass balance using the regional climate model MAR (1979–2015) and identification of
319 dominant processes. *Cryosphere*, 13(1), 281–296. doi:10.5194/tc-13-281-2019
- 320 Bromwich, D. H., Nicolas, J. P., Monaghan, A. J., Lazzara, M. A., Keller, L. M., Weidner, G. A.,
321 & Wilson, A. B. (2013). Central West Antarctica among the most rapidly warming regions on
322 Earth. *Nature Geoscience*, 6(2), 139–145, doi:10.1038/ngeo1671
- 323 Buizert, C., Sigl, M., Severi, M., Markle, B. R., Wettstein, J. J., McConnell, J. R., Pedro, J. B.,
324 Sodemann, H., Goto-Azuma, K., Kawamura, K., Fujita, S., Motoyama, H., Hirabayashi, M.,
325 Uemura, R., Stenni, B., Parrenin, F., He, F., Fudge, T. J., & Steig, E. J. (2018). Abrupt ice-age
326 shifts in southern westerly winds and Antarctic climate forced from the north. *Nature*, 563(7733),
327 681–685. doi:10.1038/s41586-018-0727-5
- 328 Chan, T., Vese, L. (1999). An Active Contour Model without Edges. In: Nielsen, M., Johansen, P.,
329 Olsen, O.F., Weickert, J. (eds) Scale-Space Theories in Computer Vision. Scale-Space 1999.
330 Lecture Notes in Computer Science, vol 1682. Springer, Berlin, Heidelberg.
331 doi:10.1007/3-540-48236-9_13
- 332 Gossart, A., S. Helsen, J. T. M. Lenaerts, S. Vanden Broucke, N. P. M. van Lipzig, and N.
333 Souverijns. (2019). “An Evaluation of Surface Climatology in State-of-the-Art Reanalyses over
334 the Antarctic Ice Sheet.” *Journal of Climate*, 32 (20), 6899–6915. doi:10.1175/JCLI-D-19-0030.1

- 335 Gorodetskaya, I. V., Tsukernik, M., Claes, K., Ralph, M. F., Neff, W. D., & Van Lipzig, N. P. M.
336 (2014) The role of atmospheric rivers in anomalous snow accumulation in East Antarctica.
337 *Geophysical Research Letters*, 41(17), 6199–6206. doi:10.1002/2014GL060881
- 338 Hersbach, H., Bell, B., Berrisford, P., Biavati, G., Horányi, A., Muñoz Sabater, J., Nicolas, J.,
339 Peubey, C., Radu, R., Rozum, I., Schepers, D., Simmons, A., Soci, C., Dee, D., & Thépaut, J.-N.
340 (2018). ERA5 hourly data on single levels from 1959 to present. Copernicus Climate Change
341 Service (C3S) *Climate Data Store (CDS)*. (Accessed on 20-JUN-2022),
342 doi:10.24381/cds.adbb2d47
- 343 Maki, T. (1972). Relations between wind direction, wind velocity, air temperature and temperature
344 gradient at Syowa station. *Tenki*, 19, 365–367.
- 345 Motoyama, H., Furukawa, T., Fujita, S., Shinbori, K., Tanaka, Y., Yuansheng, L. I., Chung, J. W.,
346 Nakazawa, F., Fukui, K., Enomoto, H., & Sugiyama, S. (2015). Glaciological data collected by the
347 48th–54th Japanese Antarctic research expeditions during 2007–2013. JARE Data Reports.
348 *Glaciology*, 35, 1–44, doi:10.15094/00010905
- 349 Motoyama, H., Furukawa, T., Kumiko, G. A., Tanaka, Y., Furusaki, A., Igarashi, M., Saito, T., &
350 Kamiyama, K. (2008). Glaciological data collected by the 45th, 46th and 47th Japanese Antarctic
351 research expeditions during 2004–2007, JARE Data Reports. *Glaciology*, 34, 1–22,
352 doi:10.15094/00005005
- 353 Paolo, F. S., Fricker, H. A., & Padman, L. (17 April 2015). Ice sheets. Volume loss from Antarctic
354 ice shelves is accelerating. *Science*, 348(6232), 327–331, doi: 10.1126/science.aaa0940
- 355 Sato, K., & Hirasawa, N. (2007). Statistics of Antarctic surface meteorology based on hourly data
356 in 1957–2007 at Syowa Station. *Polar Science*, 1(1), 1–15. doi:10.1016/j.polar.2007.05.001

- 357 Suzuki, K., Shimomura, M., Nakamura, K., Hirasawa, N., Yabuki, H., Yamanouchi, T., &
358 Tokunaga, T. (2021). Identifying snowfall clouds at Syowa station, Antarctica via a convolutional
359 neural network. *Advances in Artificial Intelligence, Advances in Intelligent Systems and*
360 *Computing*. JSAI 2020. Cham: Springer, 1357, 73–83. doi:10.1007/978-3-030-73113-7_7
- 361 Suzuki, K., Yamanouchi, T., & Motoyama, H. (2008). Moisture transport to Syowa and Dome Fuji
362 stations in Antarctica. *Journal of Geophysical Research*, 113, (D24). doi:10.1029/2008JD009794
- 363 Wang, Y., Hou, S., Sun, W., Lenaerts, J. T. M., van den Broeke, M. R., & van Wessem, J. M.
364 (2015). Recent surface mass balance from Syowa Station to Dome F, East Antarctica: comparison
365 of field observations, atmospheric reanalysis, and a regional atmospheric climate model. *Climate*
366 *Dynamics*, 45(9–10), 2885–2899. doi:10.1007/s00382-015-2512-6
- 367 Zwally, H. J., Li, J., Robbins, J. W., Saba, J. L., Yi, D., & Brenner, A. C. (2015). Mass gains of the
368 Antarctic ice sheet exceed losses. *Journal of Glaciology*, 61(230), 1019–1036.
369 doi:10.3189/2015JoG15J071